

DOI:10.1002/ejic.201300816

## Quaterphenylterpyridine: Synthesis and Metal-Ion Complexation

Young Hoon Lee,<sup>[a]</sup> Akira Fuyuhiko,<sup>[b]</sup> Jack M. Harrowfield,<sup>[c]</sup>  
Yang Kim,<sup>\*[a]</sup> Alexandre N. Sobolev,<sup>[d]</sup> and Shinya Hayami<sup>[e]</sup>

**Keywords:** N ligands / X-ray diffraction / Aromatic interactions / Fluorescence spectroscopy / Zinc

A quaterphenylterpyridine ligand (qptpy) with the rodlike quaterphenyl unit attached in the 4'-position has been synthesised by a Pd-catalysed Suzuki cross-coupling reaction. A crystal structure determination on the complex [Zn(qptpy)-Cl<sub>2</sub>]-dmf (dmf = dimethylformamide) has shown the ligand to be bound in the expected N<sub>3</sub>-tridentate manner to the essentially trigonal-bipyramidal dichloro metal ion, with the quaterphenyl substituents involving a twisted array of the separate phenyl groups and the shortest contacts between aromatic

groups involving just the polar terpyridine head groups to give an infinite, offset face-to-face (OFF)  $\pi$ -stacking array. A comparison is made with the structures of the bis(ligand) complexes of Zn(ClO<sub>4</sub>)<sub>2</sub> and Cd(ClO<sub>4</sub>)<sub>2</sub> with the bromobiphenylterpyridine ligand (Brbptpy) synthesised as an intermediate for the formation of qptpy. A study of the absorption and emission spectra of qptpy and a range of its metal-ion complexes has shown that the ligand provides a ratiometric fluorescence response for both Zn<sup>II</sup> and Cd<sup>II</sup>.

### Introduction

A “push–pull” fluorophore in which electron-donating and electron-withdrawing substituents are linked by a conjugated system can display efficient intramolecular charge transfer (ICT) between the donor and the acceptor upon excitation by light, which effectively leads to a redshift of the emission from the initial excited state.<sup>[1]</sup> Metal-ion binding can result in significant enhancement of the acceptor characteristics of a ligand, and this effect has been exploited in the use of ICT fluorescence to detect and quantify various metal ions.<sup>[2]</sup> As a metal-ion binding site, the terpyridine core has received considerable attention owing to the stability of its complexes with a wide range of metal ions.<sup>[3]</sup> It has not, however, been considered a useful fluorophore in its unsubstituted form because of the need for short wavelengths for its excitation and consequently an emission

that generally only just reaches the visible region. The terpyridine platform, nonetheless, is one for which numerous methods of functionalisation are well established<sup>[4]</sup> and thus it has been possible to produce a variety of derivatives of real applicability.<sup>[5]</sup>

Various well-known fluorophores such as difluoroborazaindacene (BODIPY),<sup>[6]</sup> pyrene<sup>[7,8]</sup> and anthracene<sup>[9]</sup> have indeed been grafted to terpyridine to provide ICT-sensitive fluorophores, which, as metal-ion complexes, have found different applications. A BODIPY-functionalised terpyridine, for example, provides an extremely sensitive sensor for Zn<sup>II</sup>,<sup>[6]</sup> whereas the Zn<sup>II</sup> complex of a pyrene-appended terpyridine shows a ratiometric fluorescence change in response to phosphate anions.<sup>[7]</sup> Many other transition-metal ions have been studied for their influence upon the emissive properties of functionalised terpyridines,<sup>[5,10]</sup> and a particularly significant aspect of this work has been the demonstration that the emission characteristics might depend not only on the nature of the substituent but also upon aggregation of the complex ions induced by their substituents. These aggregation effects have been thoroughly studied for polycyclic aromatic substituents, some as large as tetraphenylethene.<sup>[11]</sup> A useful feature of such “push” components is that they are neither acidic nor basic, and thus, unlike otherwise very effective amino substituents,<sup>[12]</sup> are unaffected by changes in solution acidity.

Recognising these facts and given our demonstration of remarkable magnetic behaviour of Co<sup>II</sup> complexes of terpyridines with very long alkyl-chain substituents,<sup>[13]</sup> our objective in the present work was to characterise a terpyridine functionalised in the 4'-position with a long quaterphenyl substituent, thereby amplifying our previous

[a] Department of Chemistry & Advanced Materials, Kosin University, 194, Wachi-Ro, Yeongdo-gu, Busan 606-701, South Korea  
E-mail: ykim@kosin.ac.kr  
<http://ykim.tistory.com/>

[b] Department of Chemistry, Graduate School of Science, Osaka University, Toyonaka, Osaka 560-0043, Japan

[c] Laboratoire de Chimie Supramoléculaire, Institut de Science et d'Ingénierie Supramoléculaires, Université de Strasbourg, 8, allée Gaspard Monge, 67083 Strasbourg, France

[d] School of Chemistry and Biochemistry, M313, University of Western Australia, Crawley, WA 6009, Australia

[e] Department of Chemistry, Graduate School of Science and Technology, Kumamoto University, 2-39-1 Kurokami, Kumamoto 860-8555, Japan

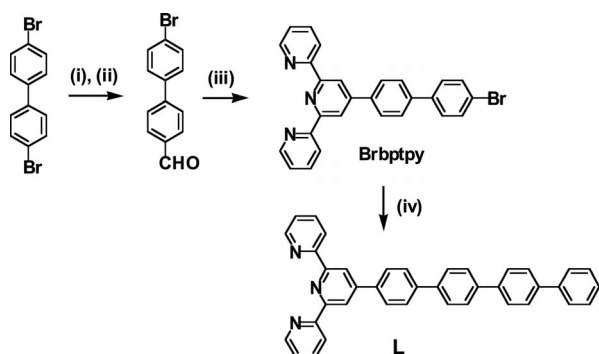
Supporting information for this article is available on the WWW under <http://dx.doi.org/10.1002/ejic.201300816>.

work<sup>[14]</sup> on the introduction of linear polyphenyl units. As a preliminary investigation of 4'-[1,1':4',1'':4'',1''']-quaterphenyl-4-yl-[2,2':6',2'']-terpyridine (qtpy), with its extended, "rigid rod" aromatic substituent, the absorption and emission spectra of the free ligand and a variety of its complexes formed with labile metal ions have been studied to establish where luminescence may be observed and whether there are appreciable metal-ion-induced redshifts in the emission. The nature of possible substituent-induced aggregation effects in the solid state has also been examined by a crystal structure determination on the complex [Zn(qtpy)Cl<sub>2</sub>]·dmf (dmf = dimethylformamide). Useful comparisons can be drawn with the structures of the bis-(ligand) complexes of Cd(ClO<sub>4</sub>)<sub>2</sub> and Zn(ClO<sub>4</sub>)<sub>2</sub> with the bromobiphenylterpyridine ligand Brbptpy formed as an intermediate for the synthesis of qtpy.

## Results and Discussion

### Syntheses

As the first step, 4'-(4'-bromobiphenyl-4-yl)-[2,2':6',2'']-terpyridine (Brbptpy) was synthesised by the reaction of 4'-bromobiphenyl-4-carbaldehyde,<sup>[15]</sup> 2-acetylpyridine, KOH and ammonia in ethanol under reflux to give a white solid. The ligand qtpy was then obtained, also as a white solid, by means of a Pd-catalysed Suzuki cross-coupling reaction of Brbptpy with biphenyl-4-boronic acid (Scheme 1). The crude product had poor solubility in common organic solvents and was purified by Soxhlet extraction into chloroform.



Scheme 1. Ligand synthesis: (i) *n*-butyllithium, THF, -78 °C; (ii) dmf, 40%; (iii) 2-acetylpyridine, NH<sub>3</sub> (aq.), KOH, EtOH, 51%; (iv) biphenyl-4-boronic acid, degassed 2 M aqueous Na<sub>2</sub>CO<sub>3</sub>, [Pd(PPh<sub>3</sub>)<sub>4</sub>], 1,2-dimethoxyethane, 71%.

Complex [Zn(qtpy)Cl<sub>2</sub>]·dmf was obtained as a white powder after reaction of L with ZnCl<sub>2</sub> in dmf. This 1:1 complex was obtained even when using a 1:2 (M/L) ratio in the reaction mixture, presumably owing to its low solubility, although since the stability constants for the binding of these metals to terpyridine are not extremely high,<sup>[3]</sup> it is possible that both [Zn(qtpy)]<sup>2+</sup> and [Zn(qtpy)<sub>2</sub>]<sup>2+</sup> species were present in the reaction mixture. It is known as well for complexes of unsubstituted terpy that the species distribution in solution is sensitive to the counter anion and ki-

netics,<sup>[16]</sup> but the use of the metal(II) perchlorates and triflates as reactants led with qtpy to the ready isolation of [M(qtpy)<sub>2</sub>](ClO<sub>4</sub>)<sub>2</sub> and [M(qtpy)<sub>2</sub>](CF<sub>3</sub>SO<sub>3</sub>)<sub>2</sub> for M = Zn, Cd. The ESI mass spectra (see the Supporting Information) of these materials in acetonitrile showed major peaks for just [ML<sub>2</sub>]<sup>2+</sup> species.

The cations [M(Brdptpy)<sub>2</sub>]<sup>2+</sup> (M = Zn, Cd) were readily crystallised as their (acetonitrile-solvated) perchlorate salts following essentially identical procedures to those used for the qtpy complexes.

### Absorption and Emission Spectroscopy of the Ligand and its Metal-Ion Complexes

The very low solubility of qtpy even in solvents of but moderate polarity rendered the study of metal-ion complexation reactions difficult, but a 1:1 mixture of CHCl<sub>3</sub> and CH<sub>3</sub>CN proved adequate for preliminary measurements on both the ligand and its complexes. For qtpy, a strong peak at 319 nm ( $\epsilon = 6.1 \times 10^4 \text{ M}^{-1} \text{ cm}^{-1}$ ) was taken to be a  $\pi$ - $\pi^*$  transition, as in the case of the parent ligand.<sup>[17]</sup> A broad emission centred about 410 nm was observed on excitation at 319 nm (Figure S1 in the Supporting Information). Consistent with an ICT origin of the fluorescence,<sup>[1,2]</sup> the emission maximum underwent a slight redshift (ca. 15 nm) with increasing solvent polarity (Figure S2 in the Supporting Information). The absorption spectrum of a dilute ( $2 \times 10^{-5} \text{ M}$ ) solution of qtpy in CH<sub>3</sub>CN/CHCl<sub>3</sub> was sensitive to the addition of an excess amount of several of the perchlorate salts of a variety of labile transition-metal ions (Cd<sup>II</sup>, Co<sup>II</sup>, Cu<sup>II</sup>, Ni<sup>II</sup>, Fe<sup>II</sup>, Fe<sup>III</sup>, Hg<sup>II</sup>, Zn<sup>II</sup>) with, as expected, addition of Fe<sup>II</sup> resulting in a dramatic colour change to violet, which was indicative of the formation of the low-spin complex.<sup>[4,5,10]</sup> Thus, the presence of a polyphenyl appendage appears to have no major detrimental influence upon the coordinating ability of the terpyridine unit.

For the same series of metal ions in a large (tenfold) excess amount over the ligand, only Zn<sup>II</sup> and Cd<sup>II</sup> caused significant modification (redshift) of the emission spectrum other than a simple diminution (quenching) of the free li-

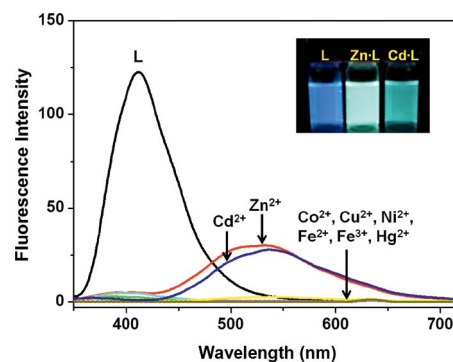


Figure 1. Fluorescence spectra of qtpy (L = 5  $\mu\text{M}$ ;  $\lambda_{\text{ex}} = 319 \text{ nm}$ ) in CHCl<sub>3</sub>/CH<sub>3</sub>CN (50:50 v/v) upon addition of 10 molar equivalents of various metal perchlorates. Inset: visual emission of qtpy, Zn<sup>II</sup>/qtpy and Cd<sup>II</sup>/qtpy solutions.

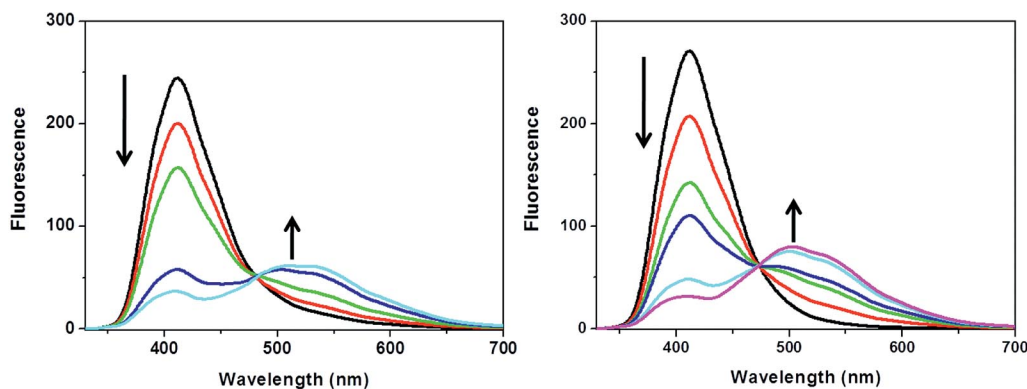


Figure 2. Fluorescence changes for qptpy (5  $\mu\text{M}$ ) upon addition of (a) 0, 0.2, 0.4, 0.8, 1.0 equiv. of  $\text{Zn}(\text{ClO}_4)_2$  and (b) 0, 0.2, 0.4, 0.6, 0.8, 1.0 equiv. of  $\text{Cd}(\text{ClO}_4)_2$  in  $\text{CH}_3\text{CN}/\text{CHCl}_3$  (1:1 v/v;  $\lambda_{\text{ex}} = 319 \text{ nm}$ ).

gand emission (Figure 1). As closed-shell species it is of course expected that  $\text{Zn}^{\text{II}}$  and  $\text{Cd}^{\text{II}}$  should not cause redox quenching, and their weaker spin-orbit coupling might explain why they do not quench ICT state luminescence to the same extent as their congener  $\text{Hg}^{\text{II}}$ .<sup>[1,2,4,5,18]</sup> (Given the high  $M/\text{qptpy}$  ratio, it is assumed that any complex present was a 1:1 species).

More precise fluorescence titrations (Figure 2) were conducted for  $\text{Zn}^{\text{II}}$  and  $\text{Cd}^{\text{II}}$  under conditions ( $L = 5 \mu\text{M}$  in  $\text{CH}_3\text{CN}/\text{CHCl}_3$ ;  $\lambda_{\text{ex}} = 319 \text{ nm}$ ) in which the ligand was initially in large excess amount over the metal ions so that presumably both  $\text{ML}_2$  and  $\text{ML}$  species were present in varying amounts throughout the titrations. For  $\text{Zn}^{\text{II}}$  (Figure 3, a) and  $\text{Cd}^{\text{II}}$  (Figure 3, b), the diminution in the ligand emission near 400 nm was accompanied by the rise of a red-shifted band with two components centred near 500 and 540 nm. The appearance of emission at a lower energy than in the ligand is consistent with metal-ion binding enhancing the “pull” character of the terpyridine terminus of the ligand in an ICT transition, and it would appear that this is so in both  $[\text{M}(\text{qptpy})]^{2+}$  and  $[\text{M}(\text{qptpy})_2]^{2+}$ .

When fluorescence spectra were recorded on solutions (5  $\mu\text{M}$ ) of the isolated  $[\text{M}(\text{qptpy})_2](\text{ClO}_4)_2$  complexes in acetonitrile, the observations were essentially identical, with some dissociation being evident from the presence of a weak band that corresponded to free ligand emission.

In the solid state (Figure 3, a), emission from the ligand was remarkably broad but, in the absence of a crystal structure determination, it is unclear why this should have been so. Emission from  $[\text{Zn}(\text{qptpy})\text{Cl}_2]$  (Figure 3, a) showed a maximum at 509 nm, a slightly shorter wavelength than that for the bis(ligand) complex  $[\text{Zn}(\text{qptpy})_2](\text{BPh}_4)_2$  (Figure 3, b), thus indicating that the bicomponent emission observed in solution might be attributed to the presence of both bis- and mono-ligand species. The emission from  $[\text{Cd}(\text{qptpy})_2](\text{CF}_3\text{SO}_3)_2$  ( $\lambda_{\text{em}} = 505 \text{ nm}$ ) indicated that in the solid state at least,  $\text{Cd}^{\text{II}}$  has a significantly weaker polarising effect on qptpy than does  $\text{Zn}^{\text{II}}$ .

The solid-state emission from the free ligand precursor to qptpy, Brbptpy, was considerably sharper than that of qptpy, but the emission from  $[\text{Zn}(\text{Brdptpy})_2](\text{ClO}_4)_2$  (Figure 4) was shifted to lower energies from that of the ligand

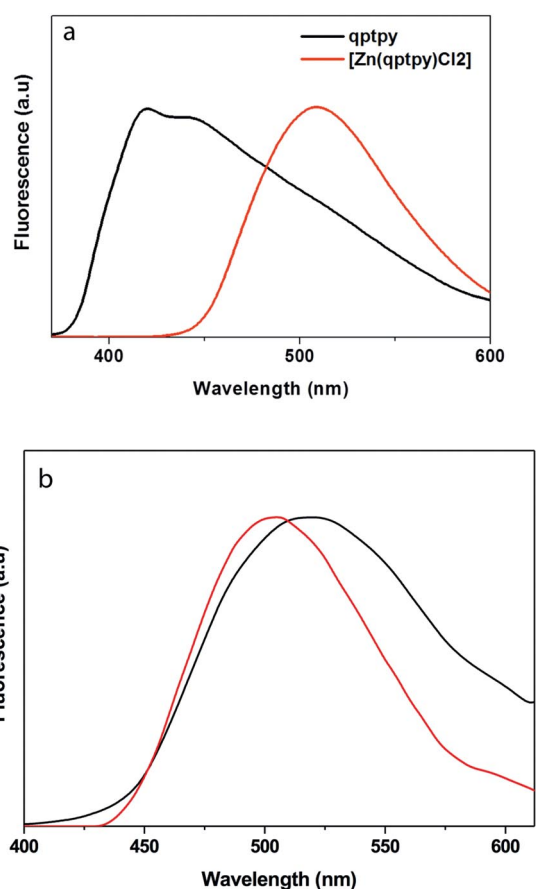


Figure 3. (a) Solid-state emission,  $\lambda_{\text{ex}} = 319 \text{ nm}$ , from qptpy (black trace;  $\lambda_{\text{em}} = 420, 439 \text{ nm}$ ) and  $[\text{Zn}(\text{qptpy})\text{Cl}_2]$  (red trace;  $\lambda_{\text{em}} = 509 \text{ nm}$ ), and (b)  $[\text{Zn}(\text{qptpy})_2](\text{BPh}_4)_2$  (black trace;  $\lambda_{\text{em}} = 520 \text{ nm}$ ) and  $[\text{Cd}(\text{qptpy})_2](\text{CF}_3\text{SO}_3)_2$  (red trace;  $\lambda_{\text{em}} = 505 \text{ nm}$ ).

by a similar amount to that seen for the qptpy complex. {The band shift for  $[\text{Cd}(\text{Brdptpy})_2](\text{ClO}_4)_2$  was again rather smaller than that of the Zn complex.} Whereas the crystal structures (see below) indicate that both the bromobiphenyl and quaterphenyl tails are twisted relative to the terpyridine head, so that delocalisation is inhibited, the (counter)polarity due to the bromo substituent appears to have a significant effect on the ICT transition energy.

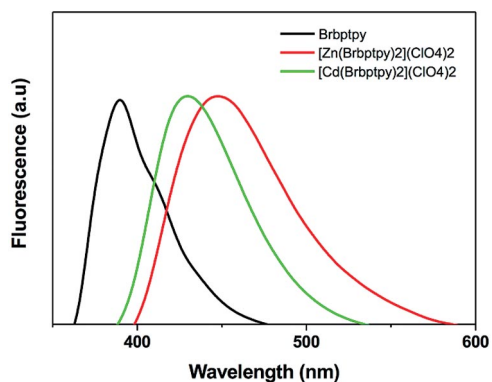


Figure 4. Solid-state fluorescence of Brbptpy (black),  $[\text{Zn}(\text{Brbptpy})_2](\text{ClO}_4)_2$  (red) and  $[\text{Cd}(\text{Brbptpy})_2](\text{ClO}_4)_2$  (green);  $\lambda_{\text{exc}}$  330 nm.

### X-ray Structure Determinations

Although 1:2 metal-ion complexes of substituted terpyridines are well known,<sup>[4,5,10,14]</sup> in the present work, with  $\text{Zn}^{\text{II}}$ , the 1:1 species  $[\text{Zn}(\text{qtpy})\text{Cl}_2]\cdot\text{dmf}$  was readily isolated in a form suitable for an X-ray structure determination, and its structure is therefore of interest in defining the metal–ligand interaction in the presence of simple anionic co-ligands. The complex ion present in this crystalline solid is a five-coordinate species with, as expected, the ligand qtpy bound in a tridentate manner through the terpyridine site and two chlorido ligands occupying equatorial sites of the essentially trigonal–bipyramidal coordination sphere (Figure 5). The structural characteristics of the  $\text{ZnN}_3$  unit are unexceptional, with the central  $\text{Zn}–\text{N}2$  bond [2.095(3) Å] significantly shorter than either bond to the flanking N donors [2.218(3); 2.208(3) Å], although all seem slightly long relative to the corresponding bond lengths in closely related  $\text{ZnL}_2$  species.<sup>[10a,14]</sup> Whereas the first phenyl unit is nearly coplanar with the central pyridine ring to which it is bound (dihedral angle ca. 3°), the other phenyl rings are all significantly tilted (dihedral angles between 30 and 45°) with respect to one another, presumably due to repulsions between hydrogen atoms.<sup>[19]</sup> Thus, at least in the solid state, conjugation is limited to that of the first phenyl ring with the terpyridine unit. In relation to forms of aggregation that might be a consequence of the introduction of a polyphenyl tail, it is interesting that the dichlorozinc–terpyridine head groups form stacked arrangements that are as prominent as the “terpyridine embrace” commonly observed in bis-(terpyridine) complexes.<sup>[10a,20]</sup> This stacking results in columnar arrays (along *c*, Figure 6), which appear to be isolated from one another by the interposition of quaterphenyl tails. This is probably an oversimplified view, since there do appear to be at least some edge-to-face (EF) contacts between tails and the terpyridine units, but it does raise the possibility that in aqueous solutions the complexes could form micelles through tail association and that this could influence their luminescence behaviour. A significant feature of the tail-to-tail contacts within the crystal is that they

are all rather remote, with the shortest being of the  $\text{CH}\cdots\pi$  type, though none are shorter than 3 Å. No  $\text{C}\cdots\text{C}$  contact is shorter than 3.5 Å. Despite the presence of the quaterphenyl tail and solvent of crystallisation, the stacking in  $[\text{Zn}(\text{L})\text{Cl}_2]\cdot\text{dmf}$  is very similar to that in  $[\text{Zn}(\text{terpy})\text{Cl}_2]$ ,<sup>[21]</sup> although in that lattice there are two slightly different stacks to form parts of infinite columns.

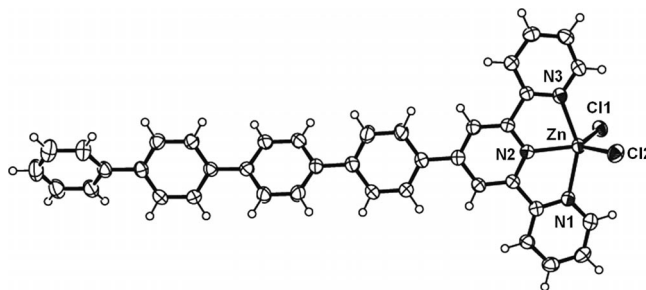


Figure 5. Molecular structure of  $[\text{Zn}(\text{qtpy})\text{Cl}_2]\cdot\text{dmf}$  with probability displacement ellipsoids plotted at the 50% level. The dmf molecule is omitted.

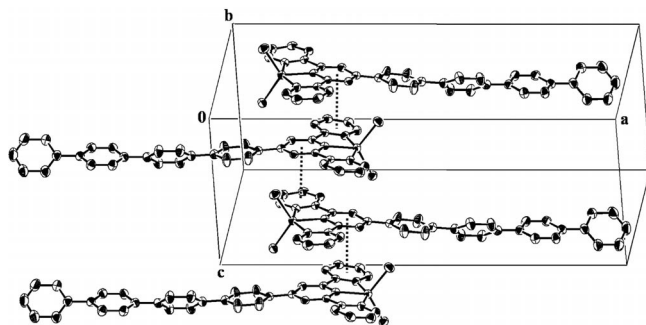


Figure 6. Packing diagram for  $[\text{Zn}(\text{qtpy})\text{Cl}_2]\cdot\text{dmf}$  showing the formation of supramolecular chains by  $\pi$ – $\pi$  interactions (dotted lines; centroid $\cdots$ centroid distance of 3.260 Å). Hydrogen atoms and dmf molecules are omitted for clarity.

The subtlety of factors that influence the solid-state structures of complexes of terpyridine and its derivatives is nicely illustrated by comparison of the structure discussed above with those of  $[\text{Zn}(\text{Brbptpy})_2](\text{ClO}_4)_2\cdot 2\text{CH}_3\text{CN}$  and  $[\text{Cd}(\text{Brbptpy})_2](\text{ClO}_4)_2\cdot\text{CH}_3\text{CN}$ . Although these two complexes have lattices that belong to the same space group, they are not isostructural, and differ very clearly in the extent to which the “terpyridine embrace” is retained. The cationic complexes within the two crystals have a very similar form (Figure 7), with the expected  $\text{MN}_6$  coordination sphere (Table 1) being slightly inflated for Cd relative to Zn and very similar, for both metals, to those in complexes of the bi- and terphenyl derivatives of terpyridine.<sup>[10a,14]</sup> Disorder within one of the terminal bromophenyl rings of the Zn complex (accompanying disorder of the perchlorate anions and one acetonitrile molecule) renders its description a little complicated, but the overall length of the cations, expressed as the terminal Br substituent separations, is 30.357(2) Å for the Zn complex (taking just the major component of

the disorder) and 30.53(1) Å for the Cd. As expected, the bromobiphenyl substituents are twisted, both internally and with respect to the terpyridine units, with dihedral angles ranging from 18 to 35° for the Zn complex (major component) and 11 to 31° for the Cd (the two substituents in each cation being inequivalent). The Br⋯M⋯Br angles are 167° (Zn; major component) and 158° (Cd), which means that the latter complex can be considered slightly more bent, the

bending in both cases being, presumably, a consequence of lattice interactions. As for the analogous complexes with simple biphenyl<sup>[10a]</sup> and terphenyl<sup>[14]</sup> substituents on the 4'-position of terpyridine, the lattices of both complexes can be considered to contain sheets of cations in which the substituents lie within these sheets. Here, however, some marked differences are apparent between the two Brdtpy complexes.

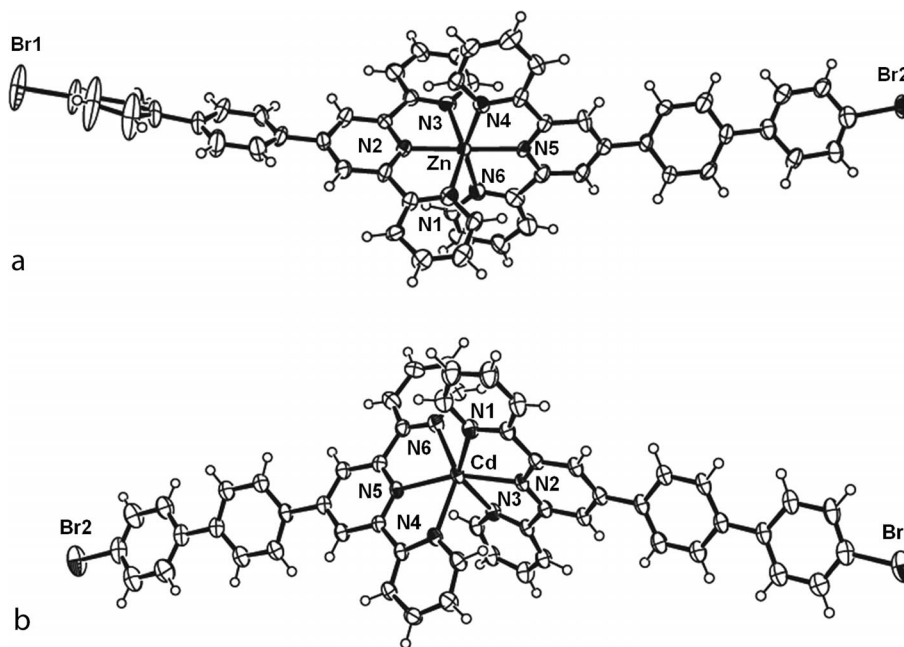


Figure 7. Molecular structure of (a)  $[\text{Zn}(\text{Brbptpy})]^{2+}$  and  $[\text{Cd}(\text{Brbptpy})]^{2+}$  cations with probability displacement ellipsoids plotted at the 50% level. Only the major component of the disordered bromophenyl ring (involving Br2) in the Zn complex is shown.

Table 1. Selected bond lengths [Å] and angles [°] for  $[\text{Zn}(\text{qtpy})\text{Cl}_2]\cdot\text{dmf}$ ,  $[\text{Zn}(\text{Brbptpy})_2](\text{ClO}_4)_2\cdot 2\text{CH}_3\text{CN}$  and  $[\text{Cd}(\text{Brbptpy})_2](\text{ClO}_4)_2\cdot\text{CH}_3\text{CN}$ .

$[\text{Zn}(\text{qtpy})\text{Cl}_2]\cdot\text{dmf}$		$[\text{Zn}(\text{Brbptpy})_2](\text{ClO}_4)_2\cdot 2\text{CH}_3\text{CN}$		$[\text{Cd}(\text{Brbptpy})_2](\text{ClO}_4)_2\cdot\text{CH}_3\text{CN}$	
Zn–N1	2.218(3)	Zn–N1	2.175(4)	Cd–N1	2.336(4)
Zn–N2	2.095(3)	Zn–N2	2.067(4)	Cd–N2	2.287(4)
Zn–N3	2.208(3)	Zn–N3	2.212(4)	Cd–N3	2.357(4)
Zn–Cl1	2.2698(10)	Zn–N4	2.175(4)	Cd–N4	2.359(4)
Zn–Cl2	2.2444(11)	Zn–N5	2.064(4)	Cd–N5	2.313(4)
		Zn–N6	2.182(4)	Cd–N6	2.305(4)
N1–Zn–N2	74.63(12)	N1–Zn–N5	105.06(15)	N2–Cd–N6	124.41(15)
N1–Zn–N3	149.17(11)	N2–Zn–N5	179.19(17)	N2–Cd–N5	160.44(14)
N2–Zn–N3	74.59(12)	N1–Zn–N2	75.74(16)	N6–Cd–N5	70.54(14)
Cl1–Zn–N1	101.91(9)	N5–Zn–N6	75.96(15)	N2–Cd–N1	70.72(14)
Cl1–Zn–N2	122.72(9)	N2–Zn–N6	104.00(15)	N6–Cd–N1	88.86(15)
Cl1–Zn–N3	93.26(8)	N4–Zn–N5	76.21(14)	N5–Cd–N1	125.63(14)
Cl2–Zn–N1	98.39(8)	N1–Zn–N4	98.60(15)	N2–Cd–N3	69.53(14)
Cl2–Zn–N2	121.48(9)	N2–Zn–N4	103.81(15)	N6–Cd–N3	102.39(15)
Cl2–Zn–N3	98.95(9)	N4–Zn–N6	152.14(14)	N5–Cd–N3	96.17(13)
Cl1–Zn–Cl2	115.63(4)	N3–Zn–N5	103.38(15)	N1–Cd–N3	137.92(14)
		N1–Zn–N3	151.51(14)	N2–Cd–N4	95.46(14)
		N2–Zn–N3	75.81(15)	N6–Cd–N4	139.79(14)
		N3–Zn–N6	95.49(15)	N5–Cd–N4	69.44(14)
		N3–Zn–N4	89.61(15)	N1–Cd–N4	111.48(15)
				N3–Cd–N4	85.63(14)

In the lattice of  $[\text{Zn}(\text{Brbptpy})_2](\text{ClO}_4)_2 \cdot 2\text{CH}_3\text{CN}$ , sheets that lie parallel to the  $bc$  plane contain the cations with their bromobiphenyl substituents lying essentially in those sheets. The distribution of the cations within these sheets resembles those found in other bis(ligand) complexes of polyphenylterpyridines,<sup>[12a,14]</sup> though with some particular characteristics (as in the other cases). Dissection of the sheets in terms of weak interactions that involve the cations can be performed in various ways, but if perchlorate  $\text{O} \cdots \text{C}$  contacts  $\leq 3.20 \text{ \AA}$  (for just the major component of the disordered anions) are taken as being indicative of significant links, then they define zigzag chains of cations, with a mean axis parallel to  $b$ , in which the  $\text{Zn} \cdots \text{Zn}$  separation is  $11.543(1) \text{ \AA}$ , with no clear direct contacts between the ligands. To form the sheet, these zigzag chains lie side by side, thereby leading to interdigitation of the bromobiphenyl tails and the formation of cation pairs in which the  $\text{Zn} \cdots \text{Zn}$  separations are either  $10.954(1)$  or  $17.1279(8) \text{ \AA}$ . (These are the only cation pairs in which part or all of another cation is not interposed.) The confrontations within these pairs lead to a number of  $\text{C} \cdots \text{C}$  contacts  $\leq 3.50 \text{ \AA}$ , but these cannot be described as reflecting true offset face-to-face (OFF) arrays in that the associated aromatic rings are far from lying parallel. In the more remote pair, one  $\text{Br} \cdots \pi$  contact [ $\text{Br}2 \cdots \text{C}42'$   $3.537(6) \text{ \AA}$ ; symmetry operation  $x, 0.5 - y, 0.5 + z$ ] bridges the two cations, but it might be that other interactions of the bromo units are more important. Thus, an alternative dissection of the lattice is to consider that the cations and their tails lie within sheets parallel to the  $ac$  plane. This is a more complicated dissection in that the separations between the sheets alternate between  $3.55$  and  $5.22 \text{ \AA}$  and it might be more appropriate to consider that the closer sheets actually constitute one undulating sheet,

but the sheets considered here are of a very simple form and provide a convenient means of distinguishing the  $\text{Zn}^{\text{II}}$  complex from its  $\text{Cd}^{\text{II}}$  analogue (see below). Thus, in one sheet in which all the Zn atoms are coplanar, the cations form a rectangular gridlike array (Figure 8, a), with the  $\text{Zn} \cdots \text{Zn}$  distances that define the sides of the rectangles being  $9.1277(8)$  and  $33.701(1) \text{ \AA}$ . The long edges are essentially defined by confronting bromobiphenyl units and involve  $\text{Br} \cdots \text{Br}$  contacts of  $3.421(1)$  (major component of disorder) and  $3.738(3) \text{ \AA}$  (minor), which might be indicative of some contribution of halogen bonding<sup>[22]</sup> to the array. The short edges, which involve the shortest  $\text{Zn} \cdots \text{Zn}$  separation of the lattice, define a vestigial "terpyridine embrace"<sup>[20]</sup> that involves two opposed pairs of peripheral pyridine rings on each cation with, in what appear to be close to true OFF contacts, a centroid  $\cdots$  centroid separation of  $3.8079(3) \text{ \AA}$ , three  $\text{C} \cdots \text{C}$  separations  $\leq 3.5 \text{ \AA}$  [ $3.408(8)$ ,  $3.431(8)$  and  $3.445(8) \text{ \AA}$ ] and two  $\text{CH} \cdots \pi$  contacts just  $< 3 \text{ \AA}$  [ $2.964(5)$ ,  $2.997(6) \text{ \AA}$ ]. Each pair within the effectively infinite chain of cations that involves these contacts is also bridged by contacts to perchlorate anions ( $\text{C} \cdots \text{O} \leq 3.20 \text{ \AA}$ ), although disorder renders the interactions difficult to describe ( $\text{O} \cdots \pi$  and/or  $\text{O} \cdots \text{HC}$ ?) and ambiguous with respect to their extent.

Despite the fairly minor dimensional differences between the  $\text{Zn}^{\text{II}}$  and  $\text{Cd}^{\text{II}}$  complex cations, the lattice of  $[\text{Cd}(\text{Brbptpy})_2](\text{ClO}_4)_2 \cdot \text{CH}_3\text{CN}$  differs markedly from that of its Zn analogue, with all vestiges of a terpyridine embrace, for example, being lost and all  $\text{Br} \cdots \text{Br}$  contacts being  $> 4.0 \text{ \AA}$ . The cations can be considered to lie in sheets, here parallel to the  $(1\ 0\ -1)$  plane (Figure 8, b), defined by their inclusion of the substituent groups, with the metal centres alternating in a slight displacement about this plane. In pro-

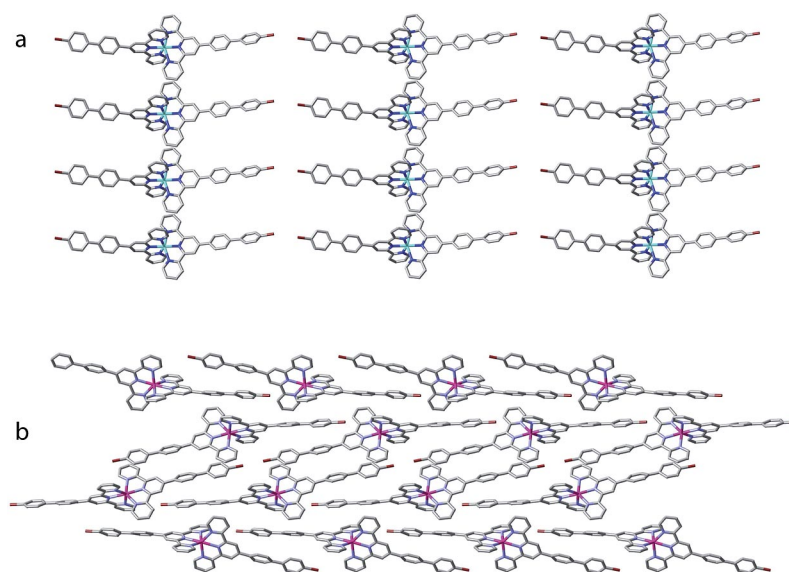


Figure 8. (a) View of a portion of one sheet of complex cations lying parallel to the  $ac$  plane in the lattice of  $[\text{Zn}(\text{Brbptpy})_2](\text{ClO}_4)_2 \cdot 2\text{CH}_3\text{CN}$ . Only the major component of the disordered bromophenyl unit is shown. (Vertical) chains involving OFF interactions and (horizontal) chains involving  $\text{Br} \cdots \text{Br}$  approaches are evident. (b) View of a portion of one sheet of complex cations lying parallel to the  $(1\ 0\ -1)$  plane in the lattice of  $[\text{Cd}(\text{Brbptpy})_2](\text{ClO}_4)_2 \cdot \text{CH}_3\text{CN}$ . Here, the shortest  $\text{Br} \cdots \text{Br}$  contacts are  $4.083(2) \text{ \AA}$ . Hydrogen atoms, solvent molecules and anions are omitted from both views; the cations are shown as stick representations.

jection onto the plane, this sheet resembles that which lies parallel to the *bc* plane in the Zn<sup>II</sup> complex lattice, and it is again possible to discern two types of cation pairs [Cd⋯Cd 15.494(6) and 19.46(1) Å] in which no other cation, in whole or in part, is interposed. The closer pair involves OFF contacts between the terminal (bromo)phenyl ring and two rings of the terpyridine head [centroid separation of 3.754(1) Å; one C⋯N contact of 3.426(6) Å plus C⋯C contacts of 3.379(6), 3.446(7) and 3.480(6) Å], whereas the more remote pair has two Br⋯HC<sub>aromatic</sub> links and two C⋯C contacts between phenyl rings that do not lie parallel to one another. As in the Zn complex sheet, zigzag chains of cations that run parallel to *b* and bridged by interactions with the perchlorate anions (defined by O⋯C contacts ≤3.20 Å) can be identified, but the Cd⋯Cd separation [14.4844(8) Å] is relatively long and is not associated with any clear aromatic⋯aromatic contacts, again as for the Zn complex. The shortest Cd⋯Cd distance [9.987(2) Å] in the sheet is associated with a pair of complex cations in which once more there is no indication of significant aromatic⋯aromatic contacts, perhaps because of the intrusion of two tails of other cation units between them, and the approach of the cations might be a consequence of bridging by a perchlorate–acetonitrile chain (O⋯HCCN⋯HC<sub>aromatic</sub>). In contrast, any two adjacent chains of cations in which the Cd⋯Cd separation is 19.46(1) Å can be considered to define a zigzag chain with a Cd⋯Cd pair separation of 11.522(4) Å, and here, despite partial intrusion of tails of other cations between the pairs, closely parallel bromophenyl and peripheral pyridine rings can be discerned, with a centroid separation of 3.7705(6) Å and four short C⋯C contacts [3.381(8), 3.428(7), 3.438(7), 3.476(8) Å], plus what might be an EF interaction that involves a bromophenyl ring and a phenyl ring bridging terpyridine and bromophenyl units. This reinforces the indication given by the consideration above of the 15.494(6) Å pair that any aromatic⋯aromatic interactions are favoured for the more polar entities (in accord with a well-known model of porphyrin stacking<sup>[23]</sup>).

The importance of ring polarisation in enhancing aromatic⋯aromatic interactions is further indicated in comparing the above two structures with those known for their analogues in which the bromo substituent is absent, [Zn(bptpy)<sub>2</sub>](BF<sub>4</sub>)<sub>2</sub> and [Cd(bptpy)<sub>2</sub>](PF<sub>6</sub>)<sub>2</sub>.<sup>[10a]</sup> Whilst the difference in anion components must have some influence, and the vestigial terpyridine embraces (i.e., peripheral pyridine⋯peripheral pyridine contacts) in these two crystals are associated with anion bridging (assuming a C⋯F contact distance of 3.20 Å to be significant), other aromatic⋯aromatic contacts, characterised by centroid⋯centroid distances <4.3 Å but not necessarily by closely parallel ring planes<sup>[10a]</sup> nor by anion bridging, appear to involve predominantly the inner phenyl ring of the tail. Its proximity to the polar terpyridine head must render it the more polar of the two substituent rings. That aromatic⋯aromatic interactions are relatively unimportant and thus subject to marked influence by seemingly minor changes in a system, however, is indicated by the fact that

in the complexes [Zn(tptpy)<sub>2</sub>](ClO<sub>4</sub>)<sub>2</sub> and [Cd(tptpy)<sub>2</sub>](ClO<sub>4</sub>)<sub>2</sub>,<sup>[14]</sup> the closest contacts to the terphenyl tail units appear to involve the terminal and next-to-terminal rings. As noted above, these comparisons involve different anions, and although it can be said that in both [Zn(bptpy)<sub>2</sub>](BF<sub>4</sub>)<sub>2</sub> and [Zn(tptpy)<sub>2</sub>](ClO<sub>4</sub>)<sub>2</sub>, for example, there is anion bridging of the closest cation pairs, the exact nature of the cation⋯anion contacts is quite different in the two cases.

## Conclusion

Introduction of a quaterphenyl chain in the 4'-position of terpyridine produces a ligand (qtpy) to give Zn<sup>II</sup> and Cd<sup>II</sup> complexes with emissive properties consistent with an ICT excited state being significantly modified in energy by the metal-ion coordination. In the solid state for the molecular dichloro-(qtpy)Zn<sup>II</sup> complex,  $\pi$  stacking of the terpyridine head groups does not appear to be perturbed by interactions with the polyphenyl tails and results in columnar arrays of the complex units very similar to those seen in the lattice of the unsubstituted ligand complex. There is segregation of the quaterphenyl tails into particular regions of the lattice, but this does not appear to be associated with  $\pi$  stacking and might at most involve some rather remote CH⋯ $\pi$  (edge-to-face) interactions. In contrast, in the cationic bis(ligand) Zn<sup>II</sup> and Cd<sup>II</sup> complexes of the precursor ligand Brbtpy found in the lattices of their perchlorate salts, significant stacking interactions that involve the substituent tails as well as the terpyridine head groups do seem to be evident. As in known structures of complexes of terpyridine with 4' bi- and terphenyl substituents, the shortest of these OFF interactions are always associated with anion bridging (through CH⋯X and/or X⋯ $\pi$  interactions), so if stacking interactions that involve single ring contacts can be attributed no more significance than that of dispersion forces,<sup>[24]</sup> the dramatic changes in aromatic⋯aromatic interaction patterns with seemingly minor changes in the cation seen in the present and related studies might be due to the very minor contribution of stacking energies to the total lattice energy and the adaptation of stacking to structures determined by more powerful forces.

## Experimental Section

**General:** All chemicals were purchased from Wako Co. and used without further purification. Elemental analyses (C,H,N) were carried out at the Instrumental Analysis Centre of Kumamoto University. <sup>1</sup>H NMR spectra were recorded with a JEOL (500-ECX) instrument (500 MHz) and Bruker 300 AM spectrometer (300.13 MHz) in deuterated solvents using TMS as internal reference. Electronic absorption and fluorescence spectra were recorded with a SCINCO S-2100 spectrophotometer and a Perkin–Elmer LS55 spectrofluorimeter, respectively. Infrared spectra were measured with a Shimadzu FTIR 8700 instrument using KBr discs.

**4'-(4'-Bromobiphenyl-4-yl)[2,2':6',2'']terpyridine (Brbtpy):** A mixture of 4'-bromobiphenyl-4-carbaldehyde (2.80 g, 10.7 mmol), 2-acetylpyridine (3.0 g, 21 mmol), KOH (1.7 g, 30 mmol) and aqueous ammonia (30%, 60 mL) in EtOH (100 mL) was heated at reflux

for 3 d to afford a dark brown solution. The mixture was evaporated to dryness under reduced pressure and the residue washed with MeOH before being purified by column chromatography on silica using ethyl acetate/hexane (1:3) to give a pale yellow powder, yield 2.54 g (51%). <sup>1</sup>H NMR (500 MHz, CDCl<sub>3</sub>): δ = 8.77 (s, 2 H, PyH<sup>3',5'</sup>), 8.73 (d, *J* = 4.0 Hz, 2 H, PyH<sup>6',6''</sup>), 8.68 (d, *J* = 7.5 Hz, 2 H, PyH<sup>3',3''</sup>), 7.99 (d, *J* = 8.0 Hz, 2 H, ArH<sup>2,6</sup>), 7.89 (t, *J* = 7.0 Hz, 2 H, PyH<sup>4,4''</sup>), 7.70 (d, *J* = 8.0 Hz, 2 H, ArH<sup>3,5</sup>), 7.59 (d, *J* = 8.0 Hz, 2 H, ArH<sup>3',5'</sup>), 7.53 (d, *J* = 8.0 Hz, 2 H, ArH<sup>2',6'</sup>), 7.36 (t, *J* = 6.0 Hz, 2 H, PyH<sup>5,5''</sup>) ppm.

**4'-[1,1';4',1'';4''',1''']Quaterphenyl-4-yl-[2,2':6',2'']terpyridine (qptpy):** Brbptpy (0.50 g, 1.1 mmol), biphenyl-4-boronic acid (0.40 g, 1.8 mmol) and [Pd(PPh<sub>3</sub>)<sub>4</sub>] (0.30 g, 0.26 mmol) were added to a three-necked round-bottomed flask under an argon atmosphere. Dimethoxyethane (50 mL) and degassed 2 M Na<sub>2</sub>CO<sub>3</sub> (25 mL, aqueous) were added, and this final mixture was heated at reflux for 48 h under argon. The solution was evaporated to dryness under reduced pressure and the black residue was extracted with ethyl acetate to remove unreacted precursors. The remaining solid was subjected to Soxhlet extraction using CHCl<sub>3</sub> for 2 d to give a pale yellow powder, yield 0.45 g (76%). <sup>1</sup>H NMR (500 MHz, CDCl<sub>3</sub>): δ = 8.75 (s, 2 H, PyH<sup>3',5'</sup>), 8.69 (d, *J* = 4.5 Hz, 2 H, PyH<sup>6',6''</sup>), 8.64 (d, *J* = 8.0 Hz, 2 H, PyH<sup>3',3''</sup>), 7.98 (d, *J* = 8.5 Hz, 2 H, ArH<sup>2,6</sup>), 7.85 (t, *J* = 7.5 Hz, 2 H, PyH<sup>4,4''</sup>), 7.76–7.68 (m, 8 H, ArH), 7.66 (d, *J* = 8.5 Hz, 2 H, ArH<sup>3',5'</sup>), 7.61 (d, *J* = 7.0 Hz, 2 H, ArH<sup>2',6'</sup>), 7.43 (t, *J* = 7.0 Hz, 2 H, ArH<sup>3'',5''</sup>), 7.32 (m, 2 H, PyH<sup>5,5''</sup> and 1 H, ArH<sup>4''</sup>) ppm.

**[Zn(Brbptpy)<sub>2</sub>](ClO<sub>4</sub>)<sub>2</sub>·2CH<sub>3</sub>CN:** Zn(ClO<sub>4</sub>)<sub>2</sub>·6H<sub>2</sub>O (0.040 g, 0.11 mmol) in dmf (5 mL) was added to a solution of Brbptpy (0.10 g, 0.22 mmol) in hot dmf (30 mL). After stirring for 6 h at 100 °C, the solvent was removed by evaporation under reduced pressure, and the white residue was washed with methanol and dried at room temperature (yield: 0.080 g). The product was dissolved in acetonitrile and diethyl ether was diffused in slowly to give colourless rodlike crystals suitable for X-ray diffraction studies. C<sub>58</sub>H<sub>42</sub>Br<sub>2</sub>Cl<sub>2</sub>N<sub>8</sub>O<sub>8</sub>Zn (1275.11): calcd. C 54.63, H 3.32, N 8.79; found C 54.58, H 3.35, N 8.84. <sup>1</sup>H NMR (300 MHz, CD<sub>3</sub>CN): δ = 9.05 (s, 2 H, PyH<sup>3',5'</sup>), 8.78 (d, *J* = 8.2 Hz, 2 H, PyH<sup>6',6''</sup>), 8.34 (d, *J* = 8.2 Hz, 2 H, PyH<sup>3',3''</sup>), 8.23 (t, *J* = 7.8 Hz, 2 H, PyH<sup>4,4''</sup>), 8.07 (d, *J* = 8.3 Hz, 2 H, ArH<sup>2,6</sup>), 7.88 (d, *J* = 4.6 Hz, 2 H, ArH<sup>3',5'</sup>), 7.81–7.75 (m, 4 H, ArH<sup>3,5</sup> and ArH<sup>2',6'</sup>), 7.46 (t, *J* = 7.5 Hz, 2 H, PyH<sup>5,5''</sup>) ppm.

**[Cd(Brbptpy)<sub>2</sub>](ClO<sub>4</sub>)<sub>2</sub>·CH<sub>3</sub>CN:** Cd(ClO<sub>4</sub>)<sub>2</sub>·H<sub>2</sub>O (0.040 g, 0.11 mmol) in dmf (5 mL) was added to a solution of Brbptpy (0.10 g, 0.22 mmol) in hot dmf (30 mL). After stirring for 6 h at 100 °C, the solvent was removed by evaporation under reduced pressure and the white residue was washed with methanol and dried at room temperature (yield: 0.07 g). The product was dissolved in acetonitrile and diethyl ether was diffused in slowly to give colourless rodlike crystals suitable for X-ray diffraction studies. C<sub>56</sub>H<sub>39</sub>Br<sub>2</sub>CdCl<sub>2</sub>N<sub>7</sub>O<sub>8</sub> (1281.08): calcd. C 52.50, H 3.07, N 7.65; found C 52.55, H 3.03, N 7.61. <sup>1</sup>H NMR (300 MHz, CD<sub>3</sub>CN): δ = 9.01 (s, 2 H, PyH<sup>3',5'</sup>), 8.82 (d, *J* = 8.2 Hz, 2 H, PyH<sup>6',6''</sup>), 8.31 (m, 4 H, PyH<sup>3',3''</sup> and PyH<sup>4,4''</sup>), 8.14 (d, *J* = 4.8 Hz, 2 H, ArH<sup>3',5'</sup>), 8.04 (d, *J* = 8.7 Hz, 2 H, ArH<sup>2,6</sup>), 7.77 (m, 4 H, ArH<sup>3,5</sup> and ArH<sup>2',6'</sup>), 7.55 (m, 2 H, PyH<sup>5,5''</sup>) ppm.

**[Zn(qptpy)Cl<sub>2</sub>]·dmf:** ZnCl<sub>2</sub> (0.030 g, 0.22 mmol) in dmf (5 mL) was added to a solution of qptpy (0.10 g, 0.19 mmol) in hot dmf (30 mL). After stirring for 6 h at 100 °C, the solvent was removed by evaporation under reduced pressure, and the white residue was washed with methanol and dried at room temperature (yield: 0.090 g). The product was dissolved in dmf and the solution was

allowed to evaporate slowly at room temperature to give colourless rodlike crystals suitable for X-ray diffraction studies. C<sub>42</sub>H<sub>34</sub>Cl<sub>2</sub>N<sub>4</sub>OZn (747.04): calcd. C 67.52, H 4.59, N 7.50; found C 67.65, H 4.48, N 7.61.

**Crystallography:** X-ray diffraction data for the single crystals were collected at 100, 153 or 200 K with a Rigaku R-Axis RAPID 191R diffractometer. Crystal evaluation and data collection were performed using Cu-K<sub>α</sub> λ = 1.54187 Å radiation with a detector-to-crystal distance of 1.91 cm. The structures were solved by heavy-atom Patterson methods<sup>[25]</sup> and expanded using Fourier techniques. The non-hydrogen atoms were refined anisotropically. Hydrogen atoms were refined using the riding model. The full-matrix least-squares refinements were based on *F*<sup>2</sup>. The absolute structures were deduced based on the Flack parameter.<sup>[26]</sup> All calculations were performed using the CrystalStructure<sup>[27]</sup> crystallographic software package except for the refinements, which were performed using SHELXL-97.<sup>[28]</sup>

**Crystal Data for [Zn(qptpy)Cl<sub>2</sub>]·dmf:** C<sub>42</sub>H<sub>34</sub>Cl<sub>2</sub>N<sub>4</sub>OZn, *M*<sub>r</sub> = 747.04; colourless crystal, size: 0.250 × 0.050 × 0.040 mm; orthorhombic, space group: *Pca*2<sub>1</sub>; *a* = 26.339(2) Å, *b* = 12.4920(2) Å, *c* = 10.7250(1) Å; *V* = 3528.8(3) Å<sup>3</sup>; *Z* = 4; *D*<sub>calcd.</sub> = 1.406 g cm<sup>-3</sup>; *F*(000) = 1544.00; μ(Cu-K<sub>α</sub>) = 26.709 cm<sup>-1</sup>; *T* = 200 K; 41795 reflections collected. Refinement of 6041 reflections (451 parameters) with *I* > 2σ(*I*) converged at final *R*<sub>1</sub> = 0.0422, *wR*<sub>2</sub> = 0.1065; GOF = 1.061.

**Crystal Data for [Zn(Brbptpy)<sub>2</sub>](ClO<sub>4</sub>)<sub>2</sub>·2CH<sub>3</sub>CN:** C<sub>58</sub>H<sub>42</sub>Br<sub>2</sub>Cl<sub>2</sub>N<sub>8</sub>O<sub>8</sub>Zn, *M*<sub>r</sub> = 1275.09; colourless crystal, size: 0.50 × 0.30 × 0.20 mm; monoclinic, space group: *P*2<sub>1</sub>/*c*; *a* = 9.1277(3) Å, *b* = 17.5802(5) Å, *c* = 33.7013(9) Å; β = 90.177(1)°; *V* = 5407.9(3) Å<sup>3</sup>; *Z* = 4; *D*<sub>calcd.</sub> = 1.566 g cm<sup>-3</sup>; *F*(000) = 2576; μ(Cu-K<sub>α</sub>) = 20.95 cm<sup>-1</sup>; *T* = 153 K; 86922 reflections collected. Refinement of 8789 reflections (800 parameters) with *I* > 2σ(*I*) converged at final *R*<sub>1</sub> = 0.0608, *wR*<sub>2</sub> = 0.1408; GOF = 1.003. The crystal used was a twin, with twin-law -1 0 0 0 -1 0 0 1. The highest residual density peak corresponded to approximately half a water molecule but this was not included in the refinement. Partial disorder was apparent in one bromophenyl group, the perchlorate anions and one of the acetonitrile molecules.

**Crystal Data for [Cd(Brbptpy)<sub>2</sub>](ClO<sub>4</sub>)<sub>2</sub>·CH<sub>3</sub>CN:** C<sub>56</sub>H<sub>39</sub>Br<sub>2</sub>CdCl<sub>2</sub>N<sub>7</sub>O<sub>8</sub>, *M*<sub>r</sub> = 1281.06; colourless crystal, size: 0.40 × 0.10 × 0.05 mm; monoclinic, space group: *P*2<sub>1</sub>/*m*; *a* = 10.4947(4) Å, *b* = 27.9850(9) Å, *c* = 18.5146(5) Å; β = 101.002(1)°; *V* = 5337.7(3) Å<sup>3</sup>; *Z* = 4; *D*<sub>calcd.</sub> = 1.594 g cm<sup>-3</sup>; *F*(000) = 2560; μ(Cu-K<sub>α</sub>) = 20.68 cm<sup>-1</sup>; *T* = 100 K; 51240 reflections collected. Refinement of 10008 reflections (685 parameters) with *I* > 2σ(*I*) converged at final *R*<sub>1</sub> = 0.0497, *wR*<sub>2</sub> = 0.1113; GOF = 1.044.

CCDC-883280 (for [Zn(qptpy)Cl<sub>2</sub>]·dmf), -936353 (for [Zn(Brbptpy)<sub>2</sub>](ClO<sub>4</sub>)<sub>2</sub>·2CH<sub>3</sub>CN) and -936354 (for [Cd(Brbptpy)<sub>2</sub>](ClO<sub>4</sub>)<sub>2</sub>·CH<sub>3</sub>CN) contain the supplementary crystallographic data for this paper. These data can be obtained free of charge from The Cambridge Crystallographic Data Centre via www.ccdc.cam.ac.uk/data\_request/cif.

**Supporting Information** (see footnote on the first page of this article): Absorption and emission spectra for qptpy in various solvents; ESI mass spectra of qptpy and its Zn<sup>II</sup> and Cd<sup>II</sup> complexes.

## Acknowledgments

This research was supported by the Basic Science Research Program of the National Research Foundation of Korea (NRF) funded by Korean Ministry of Education (2011-0011187), as well

as by the Japanese Ministry of Education, Culture, Sports, Science and Technology (MEXT) through the Innovative Areas “Coordination Programming” (area 2107).

- [1] a) Z. M. Grabowski, *Pure Appl. Chem.* **1993**, *65*, 1751–1756; b) Z. M. Grabowski, K. Rotkiewicz, *Chem. Rev.* **2003**, *103*, 3899–4031.
- [2] J. Wu, W. Liu, J. Ge, H. Zhang, P. Wang, *Chem. Soc. Rev.* **2011**, *40*, 3483–3485.
- [3] J. W. Hamilton, M. J. Anhorn, K. A. Oscarson, J. H. Reibenspies, R. D. Hancock, *Inorg. Chem.* **2011**, *50*, 2764–2770.
- [4] U. S. Schubert, H. Hofmeier, G. R. Newkome, *Modern Terpyridine Chemistry*, Wiley-VCH, Weinheim, Germany, **2006**.
- [5] Wild, A. Winter, F. Schlütter, U. S. Schubert, *Chem. Soc. Rev.* **2011**, *40*, 1459–1511.
- [6] Goze, G. Ulrich, L. Charbonnière, M. Cesario, M. Prangé, R. Ziessel, *Chem. Eur. J.* **2003**, *9*, 3748–3755.
- [7] X. Peng, Y. Xu, S. Sun, Y. Wu, J. Fan, *Org. Biomol. Chem.* **2007**, *5*, 226–228.
- [8] D’Aléo, E. Cecchetto, L. De Cola, R. M. Williams, *Sensors* **2009**, *9*, 3604–3626.
- [9] G. Albano, V. Balzani, E. C. Constable, M. Maestri, D. R. Smith, *Inorg. Chim. Acta* **1998**, *277*, 225–231.
- [10] See, for example: a) N. W. Alcock, P. R. Barker, J. M. Haider, M. J. Hannon, C. L. Painting, Z. Pikramenou, E. A. Plummer, K. Rissanen, P. Saarenketo, *J. Chem. Soc., Dalton Trans.* **2000**, 1447–1461; b) V. Guerschais, J.-L. Fillaut, *Coord. Chem. Rev.* **2011**, *255*, 2448–2457.
- [11] Y. Hong, S. Chen, C. W. T. Leung, J. W. Y. Lam, J. Liu, N.-W. Tseng, R. T. K. Kwok, Y. Yu, Z. Wang, B. Z. Tang, *ACS Appl. Mater. Interfaces* **2011**, *3*, 3411–3418.
- [12] a) W. Goodall, J. A. G. Williams, *Chem. Commun.* **2001**, 2514; b) X. Chen, Q. Zhou, Y. Cheng, Y. Geng, D. Ma, Z. Xie, L. Wang, *J. Lumin.* **2007**, *127*, 81–90; c) B. Valeur, I. Leray, *Coord. Chem. Rev.* **2000**, *205*, 3–40.
- [13] a) S. Hayami, Y. Shigeyoshi, M. Akita, K. Inoue, K. Kato, K. Osaka, M. Takata, R. Kawajiri, T. Mitani, Y. Maeda, *Angew. Chem.* **2005**, *117*, 4977; *Angew. Chem. Int. Ed.* **2005**, *44*, 4899–4903; b) S. Hayami, K. Kato, Y. Komatsu, A. Fuyuhiko, M. Ohba, *Dalton Trans.* **2011**, *40*, 2167–2169.
- [14] Y. H. Lee, E. Kubota, A. Fuyuhiko, S. Kawata, J. M. Harrowfield, Y. Kim, S. Hayami, *Dalton Trans.* **2012**, *41*, 10825–10831.
- [15] J.-C. Poupon, D. Marcoux, J.-M. Cloarec, A. B. Charette, *Org. Lett.* **2007**, *9*, 3591–3594.
- [16] a) E. C. Constable, K. Harris, C. E. Housecroft, M. Neuburger, J. A. Zampese, *Dalton Trans.* **2011**, *40*, 11441–11450; b) B. Bozic-Weber, E. C. Constable, N. Hostettler, C. E. Housecroft, R. Schmitt, E. Schönhofer, *Chem. Commun.* **2012**, *48*, 5727–5729.
- [17] K. Nakamoto, *J. Phys. Chem.* **1960**, *64*, 1420–1425.
- [18] J. S. Kim, D. T. Quang, *Chem. Rev.* **2007**, *107*, 3780–3799.
- [19] E. A. Medlycott, G. S. Hanan, *Chem. Soc. Rev.* **2005**, *34*, 1343–142.
- [20] a) M. L. Scudder, H. A. Goodwin, I. G. Dance, *New J. Chem.* **1999**, *23*, 695–705; b) J. McMurtrie, I. G. Dance, *CrystEngComm* **2005**, *7*, 216–229; c) I. G. Dance, M. L. Scudder, *CrystEngComm* **2009**, *11*, 2233–2247.
- [21] F. W. B. Einstein, B. R. Penfold, *Acta Crystallogr.* **1966**, *20*, 924–926.
- [22] a) P. Metrangelo, T. Pilati, G. Resnati, *CrystEngComm* **2006**, *8*, 946–947; b) P. Metrangelo, T. Pilati, G. Terraneo, S. Biella, G. Resnati, *CrystEngComm* **2009**, *11*, 1187–1196.
- [23] A. Hunter, J. K. M. Sanders, *J. Am. Chem. Soc.* **1990**, *112*, 5525–5534.
- [24] S. Grimme, *Angew. Chem.* **2008**, *120*, 3478; *Angew. Chem. Int. Ed.* **2008**, *47*, 3430–3434.
- [25] PATTY: P. T. Beurskens, G. Admiraal, H. Behm, G. Beurskens, J. M. M. Smits, C. Smykalla, *Z. Kristallogr. Suppl.* **1991**, *4*, 99.
- [26] H. D. Flack, *Acta Crystallogr., Sect. A* **1983**, *39*, 876–881.
- [27] *CrystalStructure*, v. 4.0, *Crystal Structure Analysis Package*, Rigaku Corporation, Tokyo 196–8666, Japan, **2000–2010**.
- [28] SHELX97: G. M. Sheldrick, *Acta Crystallogr., Sect. A* **2008**, *64*, 112–122.

Received: June 28, 2013  
Published Online: October 8, 2013